International Journal of Engineering Research-Online
A Peer Reviewed International Journal
Articles available online http://www.ijoer.in; editorijoer@gmail.com

Vol.9., Issue.4, 2021
July-August

RESEARCH ARTICLE

ISSN: 2321-7758

COMPUTATIONAL FLUID DYNAMIC ANALYSIS ON THE ENERGY DAMPENING BUILDING

S. KIRANMAIYE[1], Dr.K.JONAH PHILLIPH[2]
1Lecturer in Mathematics, Govt. Degree College, Naidupet
2Lecturer in Mathematics, T.R.R. Govt. Degree College, Kandukur
DOI: 10.33329/ijoer.9.4.43

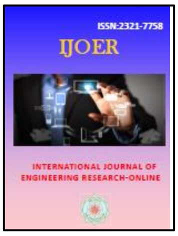

ABSTRACT

The Dam spillway building is designed with a side-channel spillway model featuring an ogee spillway type. The physical model test for the energy reducing building section utilised a modified USBR Type II flat stilling pond system. The stilling pond had a length of 31 metres and was designed to handle a flood discharge of Q100. During the test, the system was controlled by flowing a flood discharge of Q1000 and the maximum possible discharge (QPMF). The objective of this study is to analyse the hydraulic flow characteristics in a CFD-based numerical model of the energy dissipation section. Specifically, we will investigate the effects of different lengths of the stilling pool (31 m, 39 m, and 53 m) on the efficiency of energy dissipation, flow classification in the escape channel, and behaviour of fluid velocity vectors. The ultimate goal is to optimise the design of the structure for maximum dampening efficiency. Based on the results of the numerical analysis, it is evident that the energy dampening building with a stilling pool length of 39 m exhibits the highest level of damping efficiency compared to the other two models. Despite all three models generating subcritical flow in the escape-channel, the model with a stilling pool length of 39 m achieves a damping efficiency of 56.72% and a Froude number of 0.14. In contrast, the models with stilling pool lengths of 31 m and 53 m respectively have damping.

Keywords: Fluid dynamics, Dam spillway building, damping efficiency, CFD, Energy damper

Introduction

Nellore District, Andhra Pradesh state, India is a relatively dry area, with relatively few water sources. In order to meet the needs of irrigation water, raw water, power generation and flood control, the construction of the Dam is planned. Research that fluid dynamic behaviour using computer devices. The spillway building design uses a side-channel spillway model with an ogee spillway threshold type.

In the physical model test, specifically for the energy-absorbing building section, a modified USBR type II flat stilling basin system with a stilling basin length of 31 m is used and is technically planned based on the design flood discharge Q100 and controlled by flowing the flood discharge Q1000 and the maximum possible Q (QPMF).

This study focuses on the discussion of determining the optimum stilling basin length and variations in the base elevation of the stilling basin building which are carried out using an empirical approach. This study is intended to determine the flow behavior in the energy-absorbing building when the final design conditions are reviewed from the CFD approach and the recommended alternatives so that the energy-absorbing building is more optimal in terms of the efficiency of the damping that occurs, the classification of flow in the escape channel and the behavior of the fluid velocity vector.

The objective is to provide a more detailed understanding based on a CFD-based numerical model of the hydraulic behavior that occurs in the energy damping structure (stilling basin), due to variations in the elevation of the stilling basin base and the length of the stilling basin.

RESEARCH METHODOLOGY

Technical data for the prototype planning of the physical model of the Dam can be seen briefly in Table 1. The data is used to build a physical model in the laboratory.

Table 1. Tabulation of Hydrological Conditions of Dam Spillway

S.No	Description	Unit	Q_{25}	Q_{50}	Q_{100}	Q_{1000}	Q_{PMF}
1	Weir Width		Side Spillway				
2	Spill Type	m	94,2				
3	Weir Elevation	m	20,0				
4	Weir Type		Ogee				
5	Inflow Discharge	m^3/det	80.24	82.34	82.75	86.1	205.03
6	Outflow Discharge	m^3/det	20.46	21.14	21.16	23.03	67.06
7	Max. MAW Elevation	m	94.87	94.88	94.88	94,91	93.6
8	Water height above Weir	m	0.6	0.61	0.61	0.65	1.33
9	Inflow velocity	m^3/det	0.24	0.15	0.25	0.24	0.71

Data Processing

Data processing in this study was carried out in two stages, namely testing the physical model of the energy-absorbing building using a modified USBR type II flat stilling basin system with a stilling basin length of 31 m in the laboratory. Data from testing the physical model in the upstream part of the energy-absorbing building or more precisely in the launch channel, were used as input variables to build a numerical model in the CFD approach analysis with a stilling basin length of 31 m, 39 m and 53 m. The taking of the variation value of the stilling basin length was because it considered many theories of determining the length of the hydraulic jump empirically used in the planning of the stilling basin as follows:

a. Hydraulic Jump

The hydraulic jump was first investigated experimentally by Bidone, an Italian scholar, in 1818. This gave Bélanger (1828) the impetus to break down the gentle slope (subcritical) with steep (supercritical). The classification of conditions of subcritical flow, critical flow and supercritical flow is defined by the Froude number (Hager, 1992):

$$F_1 = \frac{V_1}{\sqrt{g.D_1}} \text{ ... Eq. (1)}$$

Where,

F_1 = Froude number at point 1;

V_1 = average flow velocity in the cross section (m/s) at point 1;

g = acceleration due to gravity (m/s2);

D_1 = hydraulic depth (m) at point 1.

b. Length of hydraulic jump

The length of hydraulic jump (Lj) is the distance calculated from the front surface of the hydraulic jump to a point on the surface of the wave roll that goes downstream. Several experts have tried to formulate the length of the hydraulic jump as an empirical equation as shown in Table 2.

Table 2. Several hydraulic jump length equations from previous researchers. Empirical Formula Researchers Year Riegel and Beebe Safranez Ludin and Barnes

Researcher	Empirical Formula	Year
Riegel and Beebe	$L_j \approx 5(D_2 - D_1)$	(1917)
Safranez	$L_j \approx 5{,}2D_2$	(1927)
Ludin and Barnes	$L_j = (4{,}5 - \frac{V_1}{V_C})D_2$	(1934)
Woycieki	$L_j = (D_2 - D_1)(8 - 0{,}05\frac{D_2}{D_1})$	(1934)
Smetana	$L_j \approx 6(D_2 - D_1)$	(1934)
Duma	$L_j = 5{,}2D_2$	(1934)
Aravin	$L_j \approx 5{,}4(D_2 - D_1)$	(1935)
Kinney	$L_j = 6{,}02(D_2 - D_1)$	(1935)
Page	$L_j \approx 5{,}6D_2$	(1935)
Chertousov	$L_j = 10{,}3D_1(F_1 - 1)^{0{,}81}$	(1935)
Bakhmetyef, Matske	$L_j = 5(D_2 - D_1)$	(1936)
Ivanchenko	$L_j = 10{,}6(F_1^2)^{-0{,}185}$	(1936)
Posey	$L_j \approx 4{,}5 - 7(D_2 - D_1)$	(1941)
Wu	$L_j = 10(D_2 - D_1)(F_1)^{-0{,}16}$	(1949)
Hager et al.	$\frac{L_j}{D_1} = 220.tgh(\frac{F_1 - 1}{22})$	(1992)
Marques et al.	$L_j \approx 8{,}5(D_2 - D_1$	(1997)
Simoes	$\frac{L_j}{D_2} = \frac{F_1^2 - 81{,}85F_1 + 61{,}13}{-0{,}62 - 10{,}17F_1}$	(2008)
Simoes dkk.	$L_j = 9{,}52(D_2 - D_1)$	(2012)

Source: Schulz, 2015)

The results of the Series 1/*final design* physical test

for Q_{100} obtained the following values: D_1 = 0.28 m; D_2= 6.17 m; Froude number at

D_1= 6.25. From these data, the empirical L_j length was calculated from several previous researchers using the equation.

In table 2 and the results are presented in Table 3. In order to know the location of the dominant value distribution of the variation of the hydraulic jump length theory, the histogram is depicted, as in Figure 1. Looking at the histogram, the largest frequency of the Lj value is between 33.56 m - 44.82 m.

In the physical model, it has been determined with the USBR II standard with an Lj length of 31 m, therefore the length of the 31 m stilling pond represents the value for the variation of 22.30 m - 33.56 m. Meanwhile, to represent the longest variant value, it is determined at 53 m due to consideration of the location factor of the limited energy-absorbing building. So this study will use the Lj variation with a value of (31 m, 39 m, 53 m) to find the optimum damping efficiency.

Table 3. Variation of hydraulic jump length (Lj) from previous researchers

S.No	Researcher	Year	$L_j(m)$
1	Riegel and Beebe	(1917)	29.45
2	Safranez	(1927)	32.08
3	Woycieki	(1934)	**40.63**
4	Smetana	(1934)	**35.34**
5	Aravin	(1935)	31.81
6	Kinney	(1935)	**35.46**
7	Page	(1935)	**34.55**
8	Chertousov	(1935)	11.05
9	Ivanchenko	(1935)	31.69
10	Wu	(1949)	**43.93**
11	Hager et al.	(1992)	14.43
12	Marques et al.	(1997)	50.07
13	Simoes	(2008)	**39.55**
14	Simoes dkk.	(2012)	56.07

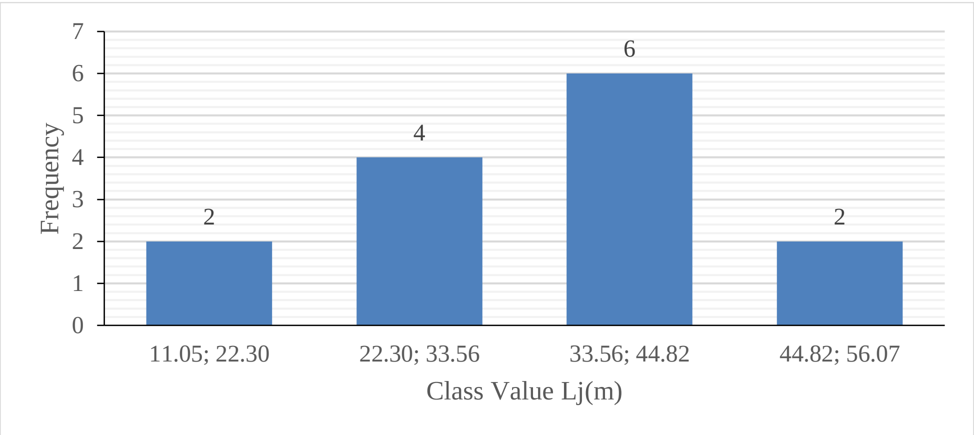

Figure 1: Histogram of Lj values from previous researchers

International Journal of Engineering Research-Online
A Peer Reviewed International Journal
Articles available online http://www.ijoer.in; editorijoer@gmail.com
Vol.9., Issue.4, 2021
July-August

The analysis work steps based on the CFD approach have three stages, including:

1. Pre-Processing: The process performed at this step is as follows

a. Creating model geometry to become a computational domain: Creating model geometry to become a computational domain using software called FLOW-3D. FLOW-3D is a general fluid dynamics computational software using numerical techniques specifically developed to solve fluid motion equations to obtain solutions in three dimensions. Fluid motion is described by non-linear, dynamic, second-order differential equations.

The numerical solution of these equations involves approximations from various forms of algebraic expressions. The resulting equations are then solved by a simulation process to produce approximate solutions to the original problem. Turbulent equation solutions that can be applied in FLOW-3D software are the k-ε, k-⍰, RNG (Re-Normalization Group) and Large Eddy Simulation equations.

The use of RNG turbulent equation solutions has several advantages compared to the k- ε turbulent equations even though they have similar standard forms, including (Babaali, 2014)

1. The RNG model has an additional form of the ε equation that significantly increases the accuracy of the results for fast fluid flow models.
2. Improved accuracy of results for flow effects that have many eddies in RNG turbulent flow modeling.
3. Fluid models with small and large Reynolds numbers can be solved well with the RNG model, while the k- ε model is only good at solving models with large Reynolds numbers.
4. The RNG model provides an analysis formula for calculating the Prandtl number, while the standard k- ε equation model uses a constant value.

b. Making mesh and grid: The model that will be made as a verification of the numerical model and physical model in this study is shown in Figure 2. This figure shows a longitudinal section of the energy absorber building that will be made into a numerical model seen from the viewpoint originating from the negative y-axis between sections 14 to 25 of the spillway building.

The treatment of this model is included in the E1-L1 notation where this model is the final design of the physical model. The first model is made based on the dimensions and sizes of the E1-L1 Series and is presented with assuming the positive direction of the x, y and z axes as shown in Figure 3.

It can be explained that the inlet is at the minimum x value or section 14 and the outlet is at the maximum x value. marked with the notation O. The model boundary condition on the maximum z-axis is air pressure marked with the letter notation P, while the letter notation W indicates the wall boundary condition.

The direction of gravity is assumed to be in the direction of the negative z-axis.

All equations used to model complex geometric areas are formulated with area functions and volume porosity functions called Fractional Area Volume Obstacle Representation (FAVORTM) and in general the FAVORTM function is based on independent time. One of the advantages of the FLOW-3D application compared to other CFD applications is its ability to define and form a good mesh from the geometric shape of the model with the application of FAVORTM (Abrari, 2015).

The creation of a mesh with a cell size of (0.25x0.25x0.25) m utilizing the FAVOR facility of the FLOW-3D software provides detailed numerical models that can represent energy-absorbing buildings well because there are no empty gaps in the geometry created (Figure 4).

International Journal of Engineering Research-Online
A Peer Reviewed International Journal
Articles available online http://www.ijoer.in; editorijoer@gmail.com
Vol.9., Issue.4, 2021
July-August

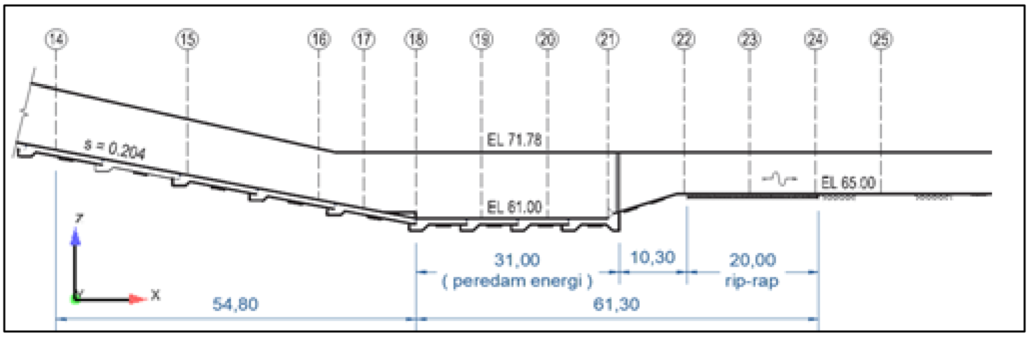

Figure 2: Section displaying the model of the energy dispensing building

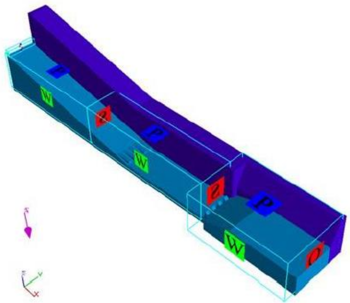

Figure 3. FLOW-3D numerical model of E1-L1 series and its boundary conditions Source: Calculation Results, 2017

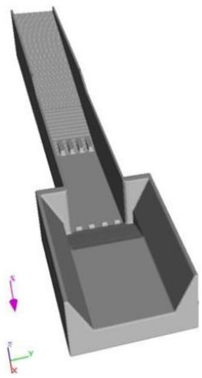

Figure 4. FAVOR mesh results of the E1-L1 Series numerical model Source: Calculation Results, 2017.

c. Defining fluid properties and other boundary condition materials: The equivalent surface roughness value that is uniformed is usually represented by the Manning coefficient value. Flow-3D software uses the Nikuradse roughness type value which has a long dimension, so it needs to be converted using Equation (2) Yen, (1991):

$$k_s = \left(n \frac{m^{\frac{1}{6}}}{0.0389} \right)^6$$

Where:

n = Manning coefficient value;

m = has a value of 1 in if the unit is meters.

d. Solver *settings (numerical scheme, convergence controls, convergence monitors, etc.)*

2. Solution (solver execution)

At this stage, the equations to be used in the CFD simulation are solved iteratively until a convergent condition is achieved. The level of accuracy of the solver is determined by, among others, the accuracy of the boundary conditions or assumptions used, meshing and numerical errors (either due to software limitations or due to user error of the software). These equations include:

a. Mass continuity equation: In general, the mass continuity equation in FLOW-3D software for incompressible flow problems with a constant ρ value in Cartesian coordinates is written as follows:

$$V_F \frac{\partial\rho}{\partial t} + \frac{\partial}{\partial x}(uA_x) + \frac{\partial}{\partial y}(uy) + \frac{\partial}{\partial z}(uA_z) = \frac{P_{SQR}}{\rho}$$

(Eq3)

Where

V_F is the ratio of open volume to fluid flow, ρ fluid density, P_{SOR} source mass. Velocity components (*u, v, w*) in the coordinate direction *(x, y, z)*. A_x denotes the ratio of open area to flowed area in the x-axis, as well as A_y and A_z in the y- and z-axes.

b. Momentum Equation: The general equation of fluid motion for fluid velocity components *(u, v, w)* in three coordinate directions is the Navier-Stokes Equation with some additions:

$$\frac{\partial u}{\partial t} + \frac{1}{V_F}\left(uA_x\frac{\partial u}{\partial x} + vA_y\frac{\partial u}{\partial y} + wA_z\frac{\partial u}{\partial z}\right) = -\frac{1}{\rho}\frac{\partial P}{\partial x} + G_x + f_x$$

$$\frac{\partial v}{\partial t} + \frac{1}{V_F}\left(uA_x\frac{\partial v}{\partial x} + vA_y\frac{\partial v}{\partial y} + wA_z\frac{\partial v}{\partial z}\right) = -\frac{1}{\rho}\frac{\partial P}{\partial y} + G_y + f_y$$

$$\frac{\partial w}{\partial t} + \frac{1}{V_F}\left(uA_x\frac{\partial w}{\partial x} + vA_y\frac{\partial w}{\partial y} + wA_z\frac{\partial w}{\partial z}\right) = -\frac{1}{\rho}\frac{\partial P}{\partial w} + G_z + f_z \quad \text{(Eq.4)}$$

In Equation (4), the variable P is the fluid pressure, while the variables *(G_x, G_y, G_z)* are the values of body accelerations formed due to the acceleration of fluid flow, *(f_x, f_y, f_z)* are the acceleration of viscosity.

3. Post *Processor*

In this step, the results of the numerical computations are visualized and documented. If necessary, further testing is carried out to obtain more accurate results to answer questions about the suitability of the model geometry, fulfillment of boundary conditions and adequacy of *mesh* size.

Hydraulic Behavior Analysis: After conducting simulations with the numerical model, several hydraulic behavior analyses will be considered based on several theories as follows:

a. Energy loss: Energy loss in a jump has the meaning of the difference in specific energy before the jump and after the jump (Peterka, 1984), the amount of which is:

$$E_1 = D_1 + \frac{V_1^2}{2g}$$

and

$$E_1 = D_1 + \frac{V_1^2}{2g}$$

for

$E_L = E_1 - E_2$.............(Eq.5)

where:

E_L = high pressure energy loss at hydraulic jump (m)

b. Energy Efficiency: The efficiency of energy loss is arranged with the following equation (Peterka, 1984):

$\frac{E_L}{E_1} = \frac{(E_1 - E_2)}{E_1}$ x 100% ....(Eq. 6)

The value of Equation (3) in percentage is used to show how much the energy-absorbing building is capable of functioning. The larger the percentage, the better the result.

c. Oblique Jump: When the flow moves obliquely, the location of the jump will vary according to the flow rate, as in flood currents. Oblique jump, is a jump in a channel with a positive slope upstream and horizontal downstream. Kindsvater (1944) classified jumps based on the relative position of the start of the jump to the floor bend, as follows (Hager, 1992):

1. Jump A, the start of the jump is at the floor bend.
2. Jump B, is between jumps A and C
3. Jump C, the last turn is above the floor
4. Jump D, the entire turn is in the oblique flow section

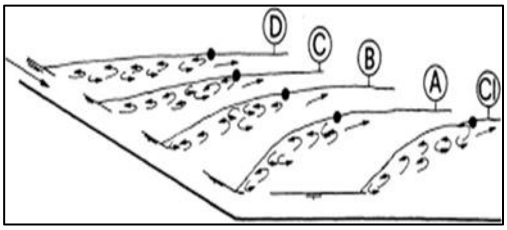

Figure 5. Types of oblique jump flow Source: Hager, 1992

International Journal of Engineering Research-Online
A Peer Reviewed International Journal
Articles available online http://www.ijoer.in; editorijoer@gmail.com
Vol.9., Issue.4, 2021
July-August

RESULTS AND DISCUSSION

Velocity Analysis Results

The results of the velocity analysis are grouped into discharge, the profile is presented in Figure 6. In general, the effect of changing the length of the stilling basin from 31 m, 39 m and 53 m causes the flow velocity in the escape channel section to decrease. For the design discharge of the Q100 energy-absorbing building, respectively, The velocity values obtained from the numerical model are: 0.697 m/s; 0.620 m/s; 0.594 m/s. This proves that increasing the length of the stilling basin reduces the flow velocity in the *escape channel.*

Water depth profile analysis results.

The results of the flow depth analysis are grouped into the length of the stilling basin, the profile of which is presented in Figure 7. Changes in the length of the stilling basin affect the flow depth downstream of the energy damping structure (escape channel).

The length of the stilling basin from 31 m, 39 m and 53 m causes the flow depth in the escape channel section to decrease from 2.247 m to 2.134 m; and 2.784 m. For the length of the stilling basin with 53 m, the highest value is produced, this is possible because the escape channel in this model is the shortest, so that further research can be done on the effect of the variable length of the *escape channel.*

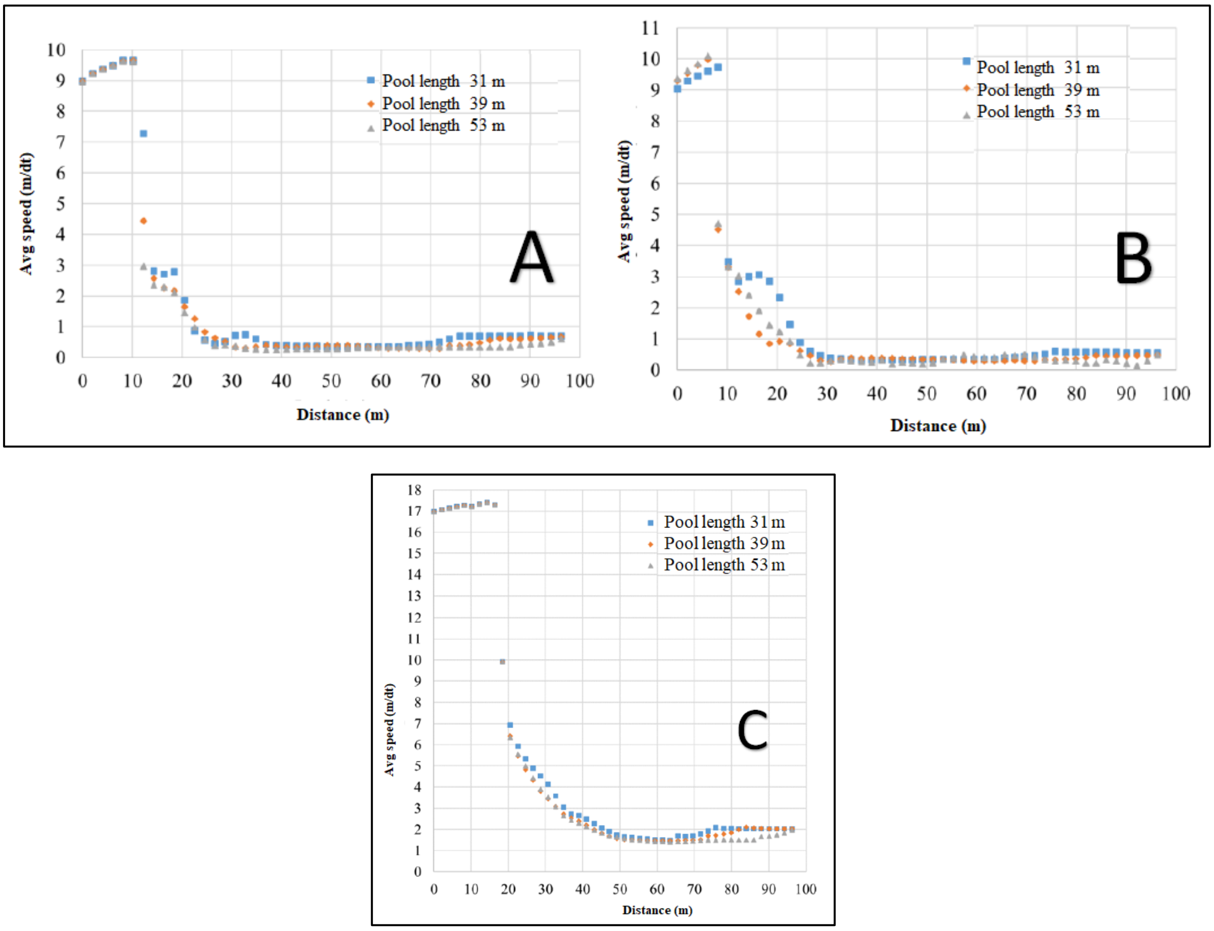

Figure 6. Velocity Profiles (a) Q100, (b) Q1000, (c) QPMF

Froude Number Analysis Results.

The Froude number analysis results (Figure 8) are grouped into the length of the stilling basin. Because the Froude number is a function of velocity, the analysis results have the same trend as the velocity analysis results. The values obtained are: 0.15; 0.14; 0.11 so that all models provide subcritical results in the escape channel section. These results are in accordance with what is desired for an energy-absorbing building design.

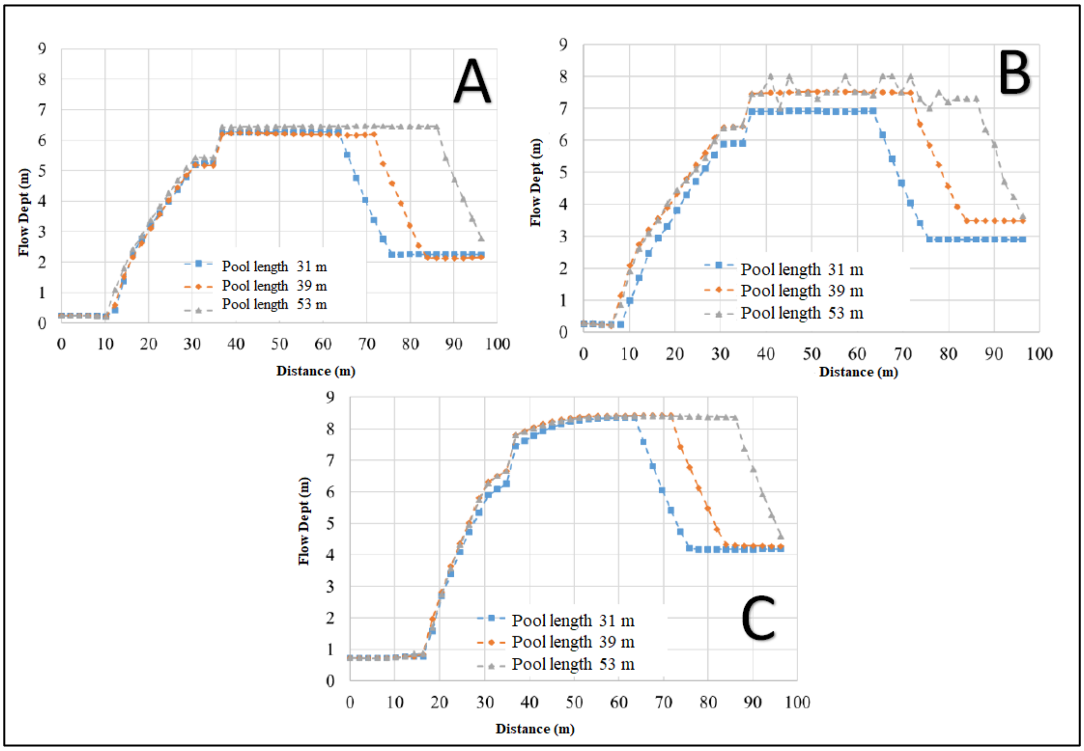

Figure 7. Flow Depth Profile (a) Q100, (b) Q1000, (c) QPMF

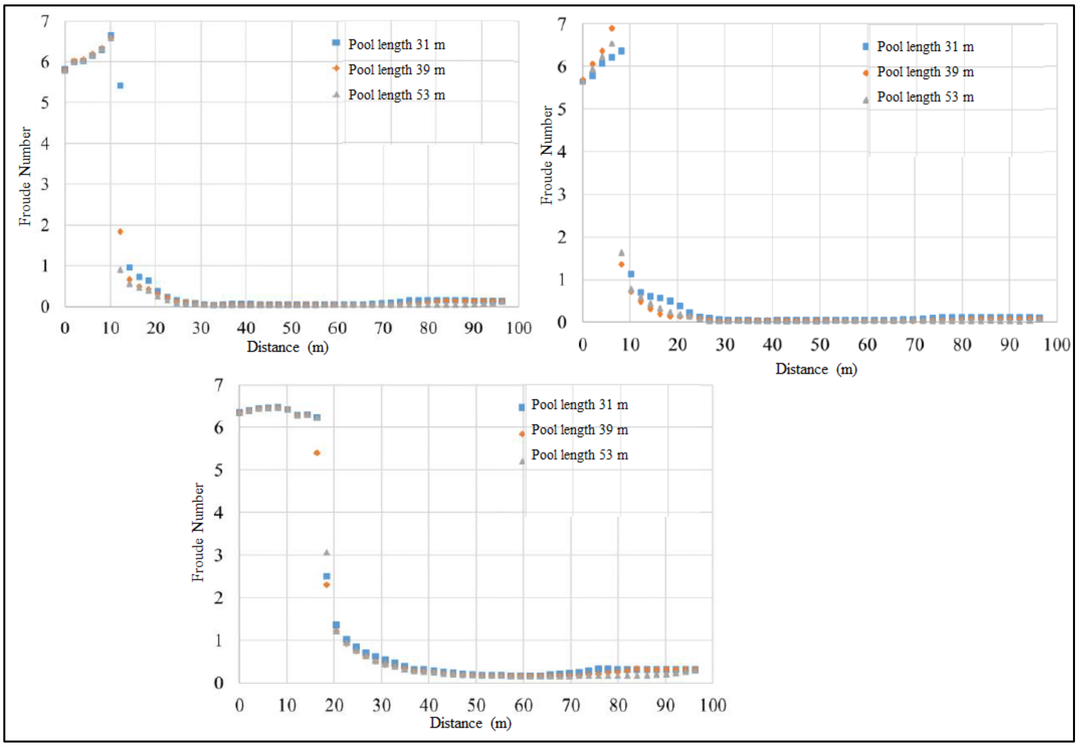

Figure 8. Profil Bilangan Froude (a) Q100 (b) Q1000 (c) QPMF

International Journal of Engineering Research-Online
A Peer Reviewed International Journal
Articles available online http://www.ijoer.in; editorijoer@gmail.com
Vol.9., Issue.4, 2021
July-August

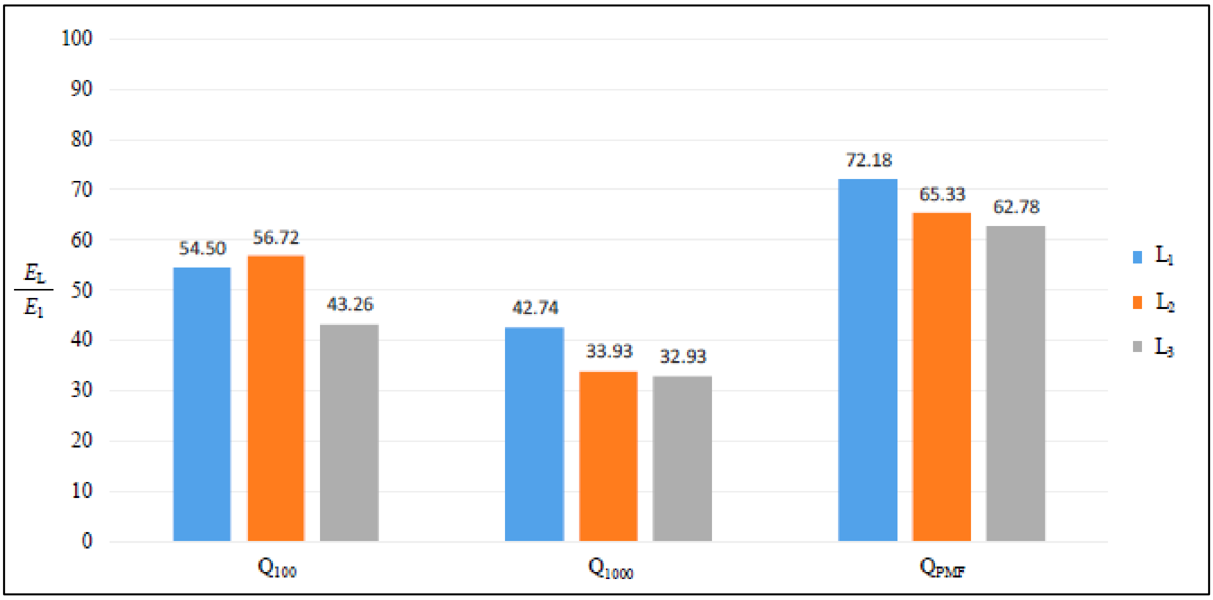

Figure 9. graph $\frac{E_L}{E_1}$ for Q100, Q1000, and QPMF debits

One of the advantages of using a numerical model is its ability to capture the velocity vectors that occur in fluid flow, so that the fluid behaviour Based on the results of the analysis above, it can be concluded that the design criteria for energy damping structures are met for all models with all simulated discharge variations.

Energy Damping Model Performance

The comparison of energy loss due to jumps with the initial energy before experiencing a jump describes the performance of the energy damper. The greater the percentage value, the better the energy damping can be said.

The calculation of the value of each percentage based on the model and discharge treatment, as well as the magnitude of the Froude number that describes the flow form category at the escape-channel location, is presented in Table 4 and Figure 9.

All model treatments have subcritical flow (F <1) downstream of the energy damping structure for the design discharge Q100, so it can be said to meet the design criteria (Table 4). The highest efficiency value of 56.72% when the discharge Q100 was obtained when the stilling basin length was 39m (Figure 9).

One of the advantages of using a numerical model is its ability to capture the velocity vector that occurs in fluid flow, so that further fluid behaviour can be studied to obtain the most optimal design from all model alternatives. Illustrations of the velocity vector are presented in Figures 10, 11 and 12.

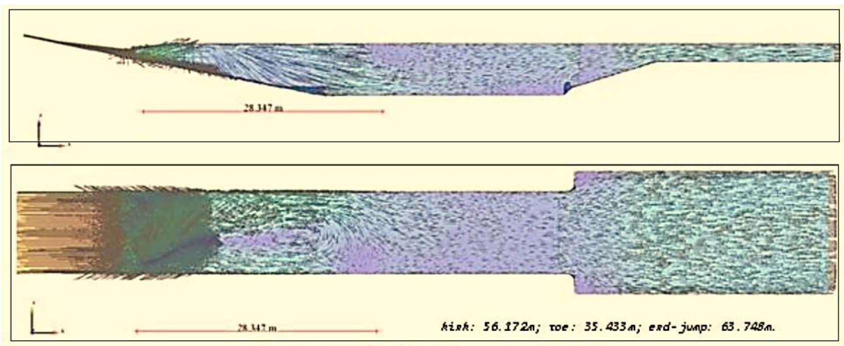

Figure 10: Velocity vectors (E_1-L_1)

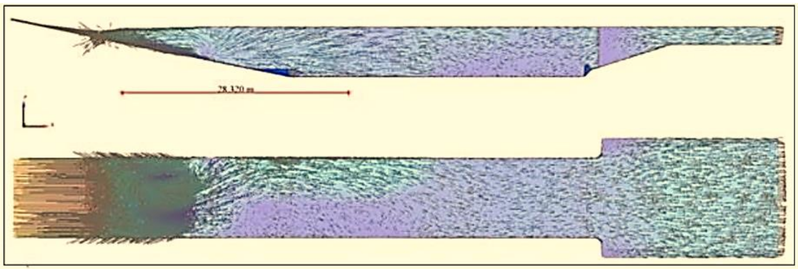

Figure 11: Velocity vectors (E_1-L_2)

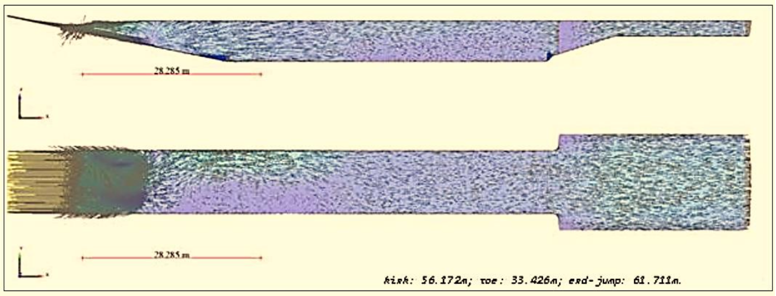

Figure 11: Velocity vectors (E_1-L_3)

Table 4. Comparison of energy lost due to the jump with energy before the jump.

No.	Debit	Period Notation	*Q* m/dt	D_1 m	D_2 m	V_1 m/dt	V_2 m/dt	$\frac{E_L}{E_1}$ %	F
1	**Physical Model**	Q_{100}	21.16	0.25	2.04	10.16	0.87	62.30	0.19
		Q_{1000}	23.03	0.44	2.77	12.59	0.87	67.04	0.17
		Q_{PMF}	67.06	0.73	3.87	16.34	1.74	71.94	0.28
2	**E_1-L_1**	Q_{100}	21.16	0.244	2.247	9.651	0.697	54.50	0.15
		Q_{1000}	23.03	0.262	2.899	9.734	0.586	42.74	0.11
		Q_{PMF}	67.06	0.729	4.209	17.266	2.088	72.18	0.32
3	**E_1-L_2**	Q_{100}	21.16	0.219	2.134	9.658	0.620	56.72	0.14
		Q_{1000}	23.03	0.213	3.485	9.978	0.452	33.93	0.08
		Q_{PMF}	67.06	0.842	4.333	15.542	2.119	65.33	033
4	**E_1-L_3**	Q_{100}	21.16	0.218	2.784	9.622	0.594	43.26	0.11
		Q_{1000}	23.03	0.243	3.632	10.088	0.471	32.93	0.07
		Q_{PMF}	67.06	0.861	4.606	15.373	1.972	62.78	0.29

The velocity vector in Figure 10 with a stilling basin length of 31 m shows a strong horizontal vortex flow at the location where the hydraulic jump occurs. The flow pattern along the stilling basin is slightly crossed. The length of the hydraulic jump is 28.315 m with a hydraulic jump type B.

The velocity vector of the model with a stilling basin length of 39 m in Figure 11 shows a flow pattern along the stilling basin that is slightly crossed and then has a stable pattern until it reaches the escape channel. The length of the hydraulic jump that occurs is 28.320 m with a hydraulic jump type B.

In Figure 12 the model has a stilling basin length of 53 m, the velocity vector describes a relatively stable flow pattern along the energy damper channel to the escape channel. The length of the hydraulic jump that occurred was 28.285 m with hydraulic jump type B.

Conclusion

After analysing the calculations and testing on the physical model of the spillway building with a scale of 1:40 and simulating with a CFD-based numerical model, the following conclusions can be drawn:

1. The recommended alternative design for an energy-absorbing building is a flat stilling basin system energy-absorbing building Modified USBR type II with a stilling basin length of 39 m.
2. The use of a CFD-based numerical model can assist in the design optimization process to cut costs and time, where the results of the analysis of the stilling basin length 39 m can optimize construction costs for energy-absorbing buildings because in theory the value of the jump length ranges from 11.05 m to 56.07 m.
3. The comparison of energy lost due to the jump with the energy before the jump when the Q100 discharge is 56.72%, the Q1000 discharge is 33.93% and the QPMF discharge is 65.33%. In the escape channel, subcritical flow occurs with a Froude number of 0.14 for the Q100 discharge; 0.08 for the Q1000 discharge and 0.33 for the QPMF discharge. The hydraulic jump that occurs is type B with a length of 28.320 m.

Suggestion

Further research on CFD-based turbulent numerical models is recommended to study in depth the determination of the starting point of the hydraulic jump (toe), the end point of the flow vortex (end-roller) that occurs, the effect of trapped air (air entrapment) in the flow and the effect of bubbles. Because, until now there has been no definite numerical method in determining these variables other than visual observation.

References

[1]. Abrari, L., Talebbeydokhti, N., and Sahraei, S., 2015, Investigation of Hydraulic Performance of Piano Shaped Weirs Using Three Dimensional Numerical Modeling, Iranian Journal of Science and Technology, Transactions of Civil Engineering Volume 39 Number C2 pp 539-558, Iran: Shiraz University.

[2]. Babaali H., Shamsai A., Vosoughifar H., 2014, Computational Modeling of the Hydraulic Jump in the Stilling Basin with Convergence Walls Using CFD Codes, Arabian Journal for Science and Engineering Volume 40, Issue 2, pp 381–395, Springerlink.com

[3]. Bayon A., Valero D., García-Bartual R., Vallés-Morán F. J., López-Jiménez P.A., 2016, Performance assessment of OpenFOAM and FLOW-3D in the numerical modeling of a low Reynolds number hydraulic jump, Environmental Modelling & Software Volume 80 pp 332-335, Elsevier Ltd.

[4]. Chow, Ven Te. 1992. Open Channel Hydraulics, translated by E.V. Nancy Rosalina. English: Hagger, Willi H., 1992, Energy Dissipators And Hydraulic Jump, Springer- Science+Business Media, B.V.

[5]. Peterka, A. J., 1984, Hydraulic Design of Stilling Basins and Energy Dissipators, United States Department of The Interior Bureau of Reclamation.

[6]. Schulz, Harry Edmar; Nobrega, Juliana Dorn; Simones, Andre Luiz Andrade; Schulz, Henry; and Porto, Rodrigo de Melo., 2015, Hydrodynamics: Concepts and Experiments, Croatia InTech.

[7]. Yen, Ben Chie (1991)., Channel flow resistance: centennial of Manning's formula, Water Resources Publications.